

RESEARCH ARTICLE

Identification of STAM1 as a novel effector of ventral projection of spinal motor neurons

Heejin Nam and Seunghee Lee*

ABSTRACT

During spinal cord development, motor neuron (MN) axons exit the spinal cord ventrally, although the molecular basis for this process remains poorly understood. STAM1 and HRS form a complex involved with endosomal targeting of cargo proteins, including the chemokine receptor CXCR4. Interestingly, the absence of CXCR4 signaling in spinal MNs is known to result in improper extension of the axons into the dorsal side of the spinal cord. Here, we report that the MN-specific ISL1-LHX3 complex directly transactivates the *Stam1* gene and that STAM1 functions in determining the ventral spinal MN axonal projections. STAM1 is co-expressed with HRS in embryonic spinal MNs, and knockdown of STAM1 in the developing chick spinal cord results in downregulation of CXCR4 expression, accompanied by dorsally projecting motor axons. Interestingly, overexpression of STAM1 or CXCR4 also results in dorsal projection of motor axons, suggesting that proper CXCR4 protein level is necessary for the ventral motor axon trajectory. Our results reveal a crucial regulatory axis for the ventral axonal trajectory of developing spinal MNs, consisting of the ISL1-LHX3 complex, STAM1 and CXCR4.

KEY WORDS: Motor neuron, ISL1, LHX3, STAM1, HRS, CXCR4, Spinal cord, Transcription, LIM complex, Mouse, Chick

INTRODUCTION

In the vertebrate central nervous system (CNS), developing neurons extend axons and find their final destination depending on guidance cues, such as attractive or repellent signaling molecules (Kolodkin and Tessier-Lavigne, 2011). Determination of axonal trajectories influences neural circuit formation and early mistakes in axon pathfinding choice take axons away from their proper targets. Among numerous neuronal subtypes generated within the CNS, only motor neurons (MNs) select a peripheral environment for axonal extension (Tosney and Landmesser, 1985). Within the hindbrain and spinal cord, newly generated MNs send their axons along one of two major trajectories, in accordance with their developmental origin and subtype identity (Guthrie and Lumsden, 1992). One set of MNs, termed ventral MNs (v-MNs), is generated at spinal cord and caudal hindbrain levels and extends axons through the ventral neural tube before emerging via a ventral exit point (Sharma et al., 1998). A second set of MNs, termed dorsal MNs (d-MNs), is generated throughout the hindbrain and at extreme rostral levels of the spinal cord and sends axons dorsally within the

neural epithelium to dorsal exit points (Sharma et al., 1998; Niederlander and Lumsden, 1996).

LIM homeobox 3 (LHX3) and Islet 1 (ISL1), two LIM-homeodomain (LIM-HD) factors, play crucial roles in directing MN fate specification and differentiation in developing spinal cord (Lee et al., 2013; Pfaff et al., 1996; Sharma et al., 1998; Tanabe et al., 1998; Thaler et al., 2002). During these processes, two ISL1:LHX3 dimers bind to nuclear LIM interactor (NLI; also known as LDB for LIM-domain binding), which has a self-dimerization domain, and form a hexameric complex, named the ISL1-LHX3 complex (Fig. 1A) (Lee et al., 2013). To understand better the role of the ISL1-LHX3 complex in spinal MN specification and differentiation, a genome-wide mapping of ISL1-LHX3 complex-binding sites has been recently performed using chromatin immunoprecipitation sequencing (ChIP-seq) (Lee et al., 2013; Mazzoni et al., 2013). These studies, combined with MN transcriptome analyses (Lee et al., 2012; Mazzoni et al., 2013), revealed that the ISL1-LHX3 complex directly regulates the expression of a wide range of downstream effector genes that function not only in cell fate specification but also in subsequent maturation steps of MN differentiation, such as cell migration, axon pathfinding and synapse formation. As a result, the roles of individual target genes of the ISL1-LHX3 complex in MN specification and differentiation/maturation have finally begun to be dissected (Cho et al., 2014; Lee et al., 2012, 2013; Mazzoni et al., 2013). Interestingly, v-MNs in embryos deficient in both LHX3 and LHX4 reorient their axonal projections dorsally, whereas the misexpression of LHX3 in d-MNs reorients their axonal projections ventrally (Sharma et al., 1998). These results strongly suggest that the ISL1-LHX3 complex also directs the ventral axonal projection of spinal MNs. However, specific target genes of the ISL1-LHX3 complex for this function have not yet been identified.

The ESCRT (endosomal sorting complexes required for transport) machinery consists of cytosolic protein complexes, known as ESCRT-0, ESCRT-I, ESCRT-II and ESCRT-III (Henne et al., 2013; Hurley, 2015). This machinery, an ancient system that buds membranes and severs membrane necks from their inner face, is involved with a variety of cellular events, including the biogenesis of multivesicular bodies in endolysosomal sorting, the budding of HIV-1 and other viruses from the plasma membrane of infected cells, the membrane abscission step in cytokinesis, the biogenesis of microvesicles and exosomes, plasma membrane wound repair, neuron pruning, extraction of defective nuclear pore complexes, nuclear envelope reformation, plus-stranded RNA virus replication compartment formation, and micro- and macroautophagy (Hurley, 2015). The ESCRT-0 complex, consisting of hepatocyte growth factor-regulated tyrosine kinase substrate (HRS; also known as HGS) and signal transducing adaptor molecule 1 (STAM1; also known as STAM) or STAM2, recognizes ubiquitylated membrane proteins during the initial step of endosomal sorting (Bache et al., 2003; Kojima et al., 2014; Mizuno et al., 2004) via the VHS

College of Pharmacy and Research Institute of Pharmaceutical Sciences, Seoul National University, Seoul 151-742, Korea.

*Author for correspondence (leeseung@snu.ac.kr)

DOI: 10.1242/dev.135848

Received 27 January 2016; Accepted 4 May 2016

(Vps27/Hrs/STAM) domain and ubiquitin-interacting motif (Mizuno et al., 2003). HRS interacts directly with STAM1/2 and suppresses the degradation of STAM1/2 (Kobayashi et al., 2005). Interestingly, *Stam1*^{-/-} mice displayed a loss of hippocampal CA3 pyramidal neurons, and STAM1 was suggested to be involved in the survival of these neurons (Yamada et al., 2001). In addition, mutations in both *Stam1* and *Stam2* result in embryonic lethality, suggesting crucial roles of STAM1 and STAM2 in embryonic development (Yamada et al., 2002).

Sorting of G protein-coupled receptors (GPCRs) into the degradative pathway plays an important role in fine-tuning the duration and magnitude of signaling. For instance, activation of the GPCR CXCR4 by its agonist ligand SDF1 (also known as CXCL12) induces its rapid ubiquitylation and sorting to lysosomes via the ESCRT machinery (Kennedy and Marchese, 2015). Interestingly, CXCR4 is expressed in the axons of v-MNs as they follow their ventral trajectory, whereas its ligand, SDF1, is expressed by mesenchymal cells surrounding the ventral neural tube (Lieberman et al., 2005; Ödemis et al., 2005; Sapede et al., 2005). Genetic studies revealed that SDF1/CXCR4 signaling directs the ventral trajectory of spinal v-MNs (Lieberman et al., 2005). Interestingly, in the absence of the SDF1/CXCR4 signaling, these neurons adopted a d-MN-like trajectory, despite preservation of their v-MN transcriptional identity (Lieberman et al., 2005). Thus, the status of CXCR4 signaling is believed to serve as a crucial determinant for the initial motor axonal trajectory and specification of v-MN connectivity (Lieberman et al., 2005), although it remains to be determined whether the role of CXCR4 in ventral projections of motor axons involves the ESCRT-dependent turnover of CXCR4.

Our findings in this report demonstrate that the ISL1-LHX3 complex directly induces expression of STAM1. We further show that STAM1 determines the ventral axonal trajectory of spinal MNs, probably through maintaining the proper amount of activated CXCR4 protein levels at a time when ventral motor axon projection is specified. Our results add regulation of the ventral-exiting spinal motor axonal projections to the list of proactive and direct roles of the ISL1-LHX3 complex in later MN maturation steps. Furthermore, our results identify STAM1 (and probably

ESCRT-0) as a crucial and novel regulator of motor axon pathfinding choice.

RESULTS

Identification of ISL1-LHX3 complex-binding sites in the *Stam1* gene

To identify novel regulators of motor axon pathfinding that function downstream of the ISL1-LHX3 complex, we analyzed genome-wide ISL1-LHX3-bound genomic loci mapped by ChIP-seq analyses (Lee et al., 2013; Mazzoni et al., 2013). Bioinformatics analysis of these ChIP-seq datasets led us to identify a series of putative direct MN target genes of the ISL1-LHX3 complex (data not shown). Among the potential direct target genes of the ISL1-LHX3 complex, *Stam1* was particularly interesting because STAM1 is known to play roles in endosomal targeting of axon guidance receptors such as CXCR4 (Marchese et al., 2003; Sierra et al., 2010; Holleman and Marchese, 2014; Bhandari et al., 2007; Malik and Marchese, 2010). This gene was associated with five ISL1-LHX3-bound ChIP-seq peaks, i.e. one binding site in the upstream promoter region and four binding sites in various introns (Fig. 1B). Within the P1 and P3 sites, we discovered a motif similar to the previously defined consensus HxRE (hexamer response element) (Fig. 1B), which is the binding site for the ISL1-LHX3 complex (Lee et al., 2008, 2013). Interestingly, P1, P4 and P5, but not P2 and P3, were highly conserved in many mammal species, but none of the five sites was conserved in chick (Fig. 1B). However, it should be noted that binding sites for the ISL1-LHX3 complex are often found in evolutionarily non-conserved regions of its target genes (Lee et al., 2013; Mazzoni et al., 2013). Overall, our results raised the possibility of *Stam1* being a direct target gene of the ISL1-LHX3 complex.

In vivo recruitment of the ISL1-LHX3 complex to *Stam1*

To test whether the ISL1-LHX3 complex is recruited to the P1–P5 regions of the *Stam1* gene *in vivo*, we performed a chromatin immunoprecipitation (ChIP) assay with antibodies against ISL1 and LHX3 using embryonic day (E) 12.5 mouse spinal cord extracts. Both ISL1 and LHX3 bound to the previously defined enhancer region in *Hb9* (also known as *Mnx1*) (Lee et al., 2008) as well as the

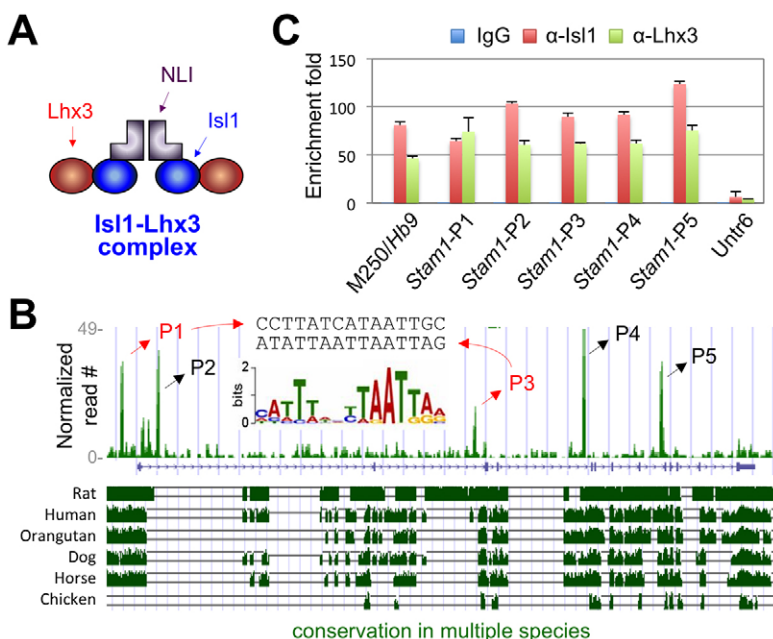


Fig. 1. ChIP-seq peaks for the ISL1-LHX3 complex in *Stam1* and their *in vivo* recruitment of the ISL1-LHX3 complex.

(A) Schematic of the ISL1-LHX3 complex. (B) Five ISL1-LHX3 complex-binding sites in *Stam1*. P1 and P3, but not P2, P4 and P5, have HxRE motifs. The sequence conservation in several species is shown below. (C) ChIP with antibodies against Isl1 and Lhx3 using E12.5 mouse embryonic spinal cord extracts, followed by quantitative PCR amplification of the P1, P2, P3, P4 and P5 regions of *Stam1* and the negative control region *Untr6*. ChIP experiments were repeated independently twice. Data are presented as the mean of duplicate values and error bars represent s.d.

P1, P2, P3, P4 and P5 regions of the *Stam1* gene but not a negative control genomic region named *Untr6* (Mali et al., 2008) (Fig. 1C). These results indicate that the endogenous ISL1-LHX3 complex is recruited to the *Stam1* gene in the developing spinal cord, validating the ChIP-seq results (Lee et al., 2013; Mazzoni et al., 2013) (Fig. 1B), and further support our proposal that the *Stam1* gene is a direct target of the ISL1-LHX3 complex in developing MNs.

Expression of STAM1 in developing spinal MNs

The binding of the ISL1-LHX3 complex to the *Stam1* gene raises the possibility that expression of STAM1 is probably induced as MNs become specified in the developing spinal cord. In support of this idea, expression of STAM1 was induced as MNs were derived from embryonic stem cells under MN differentiation conditions (Lee et al., 2012; Wichterle et al., 2002) (Fig. S1). To test this possibility further, we performed *in situ* hybridization (ISH) and immunohistochemistry (IHC) on mouse embryonic spinal cord. STAM1 began to be expressed around E9.5 (Fig. 2A) and its expression was strongly induced in MNs at E10.5 (Fig. 2B), which is soon after ISL1⁺/LHX3⁺ MNs are born. In addition, STAM1 was also expressed in the dorsal root ganglion (DRG) (Fig. 2B). By E11.5, STAM1 was expressed in the neuronal zone of the spinal cord and the DRG, but its expression remained strongest in MNs and STAM1 was continuously expressed in MNs at later stages of development (data not shown). STAM1 protein was mainly localized in the cytoplasm and axons and exhibited a punctate pattern (Fig. 2C) and was colocalized with the early endosomal marker EEA1 (Mu et al., 1995) in primary MN culture (Fig. 2D), suggesting that STAM1 protein is enriched in endosomes within MNs.

Activation of *Stam1* HxRE by the ISL1-LHX3 complex

To determine whether STAM1 expression is induced directly by the ISL1-LHX3 complex via HxREs that were identified by ChIP-seq,

we constructed a luciferase reporter and a GFP reporter linked to five copies of the HxRE of the P3 peak (Fig. 1B). In mouse embryonic P19 cells, the co-expression of ISL1 and LHX3, which form the ISL1-LHX3 complex with endogenous NLI, strongly activated the luciferase reporter, whereas the expression of ISL1 or LHX3 alone did not (Fig. 3A). To test whether the ISL1-LHX3 complex can activate the HxRE *in vivo*, we electroporated the chick neural tube with a GFP reporter linked to five copies of the P3-HxRE at a time when MNs are being specified, and found that GFP is specifically expressed in MNs (Fig. 3B, left panels). We then co-electroporated ISL1 and LHX3 expression vectors with the GFP reporter and found that co-expression of ISL1 and LHX3 activates P3-HxRE ectopically in non-MNs as shown by upregulation of GFP in the dorsal spinal cord (Fig. 3B, right panels), where HB9⁺ ectopic MNs are induced. Together, these results indicate that the ISL1-LHX3 complex directly triggers the expression of STAM1 at least in part via HxRE motifs in the *Stam1* gene during MN differentiation.

Requirement of ISL1 for STAM1 expression in MNs

To test further whether the induction of STAM1 in differentiating MNs is dependent on the action of the ISL1-LHX3 complex, we analyzed STAM1 expression in *Hb9*^{-/-}; *Isl1*^{-/-} double knockout (dKO) embryos. It has been previously shown that the expression of ISL1 is drastically reduced in postmitotic MNs of dKO embryos resulting in severely impaired motor axon projection, while retaining other basic characteristics of MNs such as expression of vesicular acetylcholine transporter (VAcHT; also known as SLC18A3) (Thaler et al., 2004). Therefore, these compound mutant embryos are expected to have impaired formation of the ISL1-LHX3 complex, providing an *in vivo* model system for the loss of ISL1-LHX3 complex function. In the spinal cord of dKO embryos, STAM1 expression in MNs was drastically reduced relative to control littermates (66% of WT; Fig. 3C), whereas STAM1 expression was relatively intact in the dorsal spinal cord

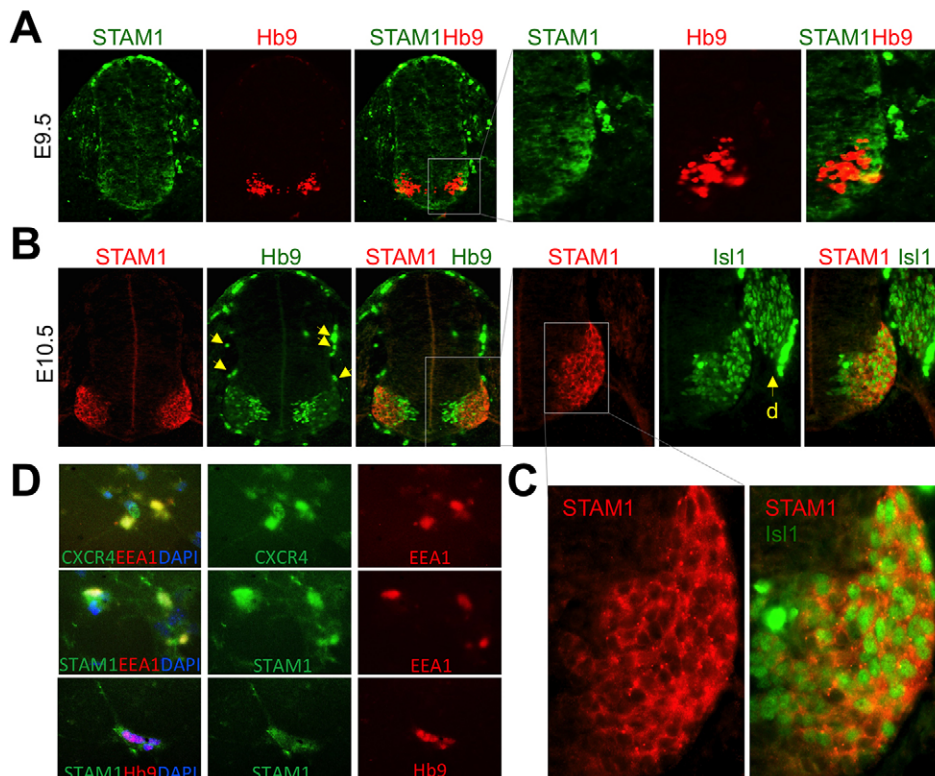


Fig. 2. Expression of STAM1 in developing spinal MNs. (A–C) Expression of STAM1 in developing MNs at E9.5 (A) and E10.5 (B,C) mouse embryos determined by IHC for STAM1, HB9 and ISL1. (C) Enlarged images highlighting the punctate patterns, which may represent endosomal expression of STAM1. (D) Colocalization of STAM1 and CXCR4 with the endosomal marker EEA1 in primary MN culture. d, dorsal root ganglion. Yellow arrows indicate non-specific blood cell signals detected.

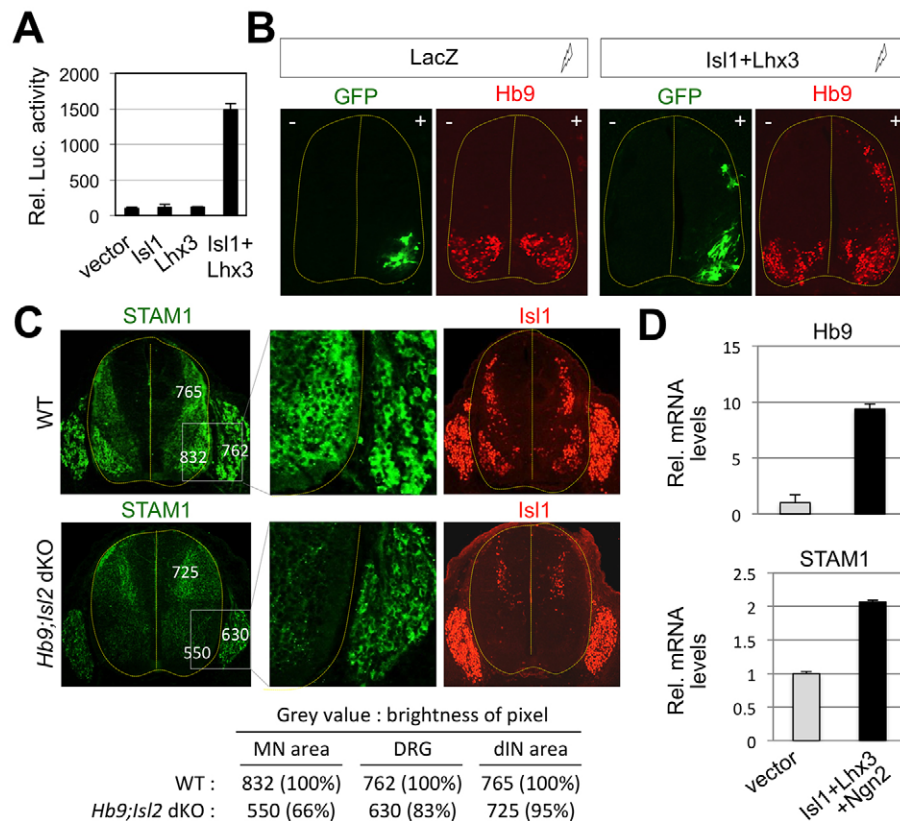


Fig. 3. *Stam1* is a target gene of the ISL1-LHX3 complex. (A) Luciferase assay for a reporter directed by five copies of P3 in *Stam1*.

Transfections were repeated independently at least three times. Data are presented as the mean of triplicate values and error bars represent s.d.

(B) *In ovo* electroporation of *lacZ* (to measure electroporation efficiency) and a GFP reporter directed by five copies of P3 in *Stam1* without or with co-expression of ISL1 and LHX3.

+, electroporated side. Experiments were repeated independently at least three times.

(C) Decreased expression of STAM1 in postmitotic MNs of E12.5 *Hb9^{-/-};Isl2^{-/-}* dKO embryos relative to control littermate embryos. Immunostaining signal intensity of STAM1 was measured in Grey value using ZEN Pro 2012. (D) Induction of STAM1 expression by the ISL1-LHX3 complex and NGN2 in P19 cells. Relative expression levels are shown as the mean of duplicate values obtained from representative experiments. Error bars represent s.d.

(95% of WT; Fig. 3C). Of note, the ISL1-LHX3 complex is not formed in the dorsal spinal cord area and expression of STAM1 in this region is expected to involve transcription factors other than the ISL1-LHX3 complex. Of note, expression of STAM1 in the DRG was also slightly dampened in the mutants in comparison with control littermates (83% of WT; Fig. 3C), suggesting that ISL1 may also control the expression of STAM1 in this region either directly or indirectly. Overall, these results further support our proposal that the ISL1-LHX3 complex plays crucial roles in the timely induction of STAM1 during MN differentiation.

Next, we tested whether the ISL1-LHX3 complex can actively induce the expression of STAM1 in P19 embryonic carcinoma cells. The proneural transcription factor NGN2 (also known as NEUROG2) has been shown to transcriptionally synergize with the ISL1-LHX3 complex to trigger MN fate specification (Lee and Pfaff, 2003). Expression of ISL1 and LHX3 (which form the ISL1-LHX3 complex with endogenous NLI) and NGN2 was capable of driving the expression of the MN marker HB9 in P19 cells (Lee and Pfaff, 2003) (Fig. 3D). Interestingly, under these conditions, the level of STAM1 expression was also significantly increased by co-expression of ISL1, LHX3 and NGN2 (Fig. 3D).

Taken together, these data support the notion that the ISL1-LHX3 complex directs the expression of STAM1 in developing MNs.

Regulation of CXCR4 levels by STAM1 in developing spinal MNs

Previous studies have shown that STAM1 and HRS form the ESCRT-0 complex, which is involved with endosomal targeting of cargo proteins including CXCR4 (Bache et al., 2003; Kanazawa et al., 2003; Kojima et al., 2014; Mizuno et al., 2003, 2004). Therefore, we hypothesized that STAM1, by forming the ESCRT-0 complex with HRS, controls the levels of CXCR4 in developing

spinal MNs. First, we confirmed the cellular association of STAM1 with HRS and CXCR4 using co-immunoprecipitation assays in HEK293 cells (Fig. 4A). HEK293 cells were transfected with HA-tagged CXCR4, Flag-tagged STAM1 and Myc-tagged HRS, pulled down with anti-HA (hemagglutinin) antibody, followed by immunoblotting to detect the association with STAM1 and HRS in the presence or absence of SDF1. SDF1 seems to enhance the stability of STAM1 and the association with CXCR4 slightly. We have also shown that STAM1, HRS and CXCR4 are relocated to endocytic endosomes in HEK293 cells when CXCR4 is activated by SDF1 (Fig. 4B). Moreover, knockdown of STAM1 using a small interfering RNA (siRNA) duplex resulted in a decrease in CXCR4 levels in HEK293 cells (data not shown). In support of our hypothesis, our IHC and ISH results revealed that HRS is co-expressed with STAM1 and CXCR4 as well as the MN marker HB9 in chick embryos at different developmental time points (Fig. 4C; Fig. S2A). The alternative SDF1 receptor CXCR7 (also known as ACKR3) was expressed in the ventricular zone of chick spinal cord but was excluded in the MN areas (Fig. S2B). Our ISH and IHC results also showed that STAM1 is co-expressed with HRS in developing MNs and other interneurons in E11.5 mouse embryos (data not shown).

Next, to determine whether reduced levels of STAM1 alters the levels of CXCR4 in developing chick spinal cord, we produced an siRNA duplex against chick STAM1 (si-STAM1) and performed *in ovo* electroporation of si-control and si-STAM1, followed by dissection of spinal cord into two halves (unelectroporated ‘–’ side versus electroporated ‘+’ side) and immunoblotting with antibodies against CXCR4 and tubulins (loading control) (Fig. 5A). We confirmed the specific reduction of STAM1 expression by si-STAM1 in chick spinal cord (Fig. S3). Similar to our results with HEK293 cells (data not shown), knockdown of STAM1 also

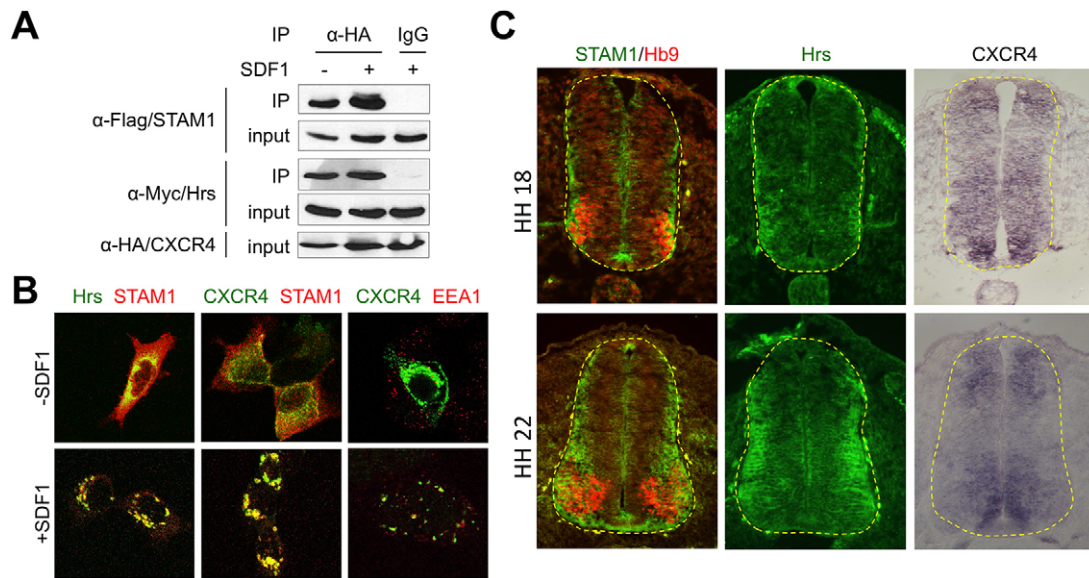


Fig. 4. Endosomal targeting of CXCR4 by STAM1 and co-expression of STAM1 and HRS in developing MNs. (A) Association of STAM1, HRS and CXCR4 in HEK293 cells. Immunoprecipitation against CXCR4 co-purified both STAM1 and HRS, and these interactions were slightly but noticeably enhanced by SDF1, the CXCR4 ligand. (B) Relocalization of STAM1, HRS and CXCR4 to endocytic endosomes in HEK293 cells in the presence of SDF1. STAM1, HRS and CXCR4 were diffuse in the cytoplasm without SDF1 but showed distinct punctate endosomal relocalization patterns marked by the endosomal marker EEA1 in the presence of SDF1. (C) Immunohistochemistry for STAM1, HB9 and HRS and ISH for CXCR4 on chick embryos at HH18–25 in adjacent sections revealed colocalization of STAM1, CXCR4 and HRS in HB9⁺ MNs. Experiments were repeated independently at least three times. Dashed lines delineate the border of the spinal cord.

decreased levels of CXCR4 whereas electroporation of si-control failed to reduce CXCR4 levels (Fig. 5B). By contrast, when we overexpressed STAM1 in one side of the chick spinal cord, expression of CXCR4 was markedly increased, suggesting that the stability of CXCR4 is regulated by STAM1 (Fig. 5B).

Taken together, these results support our hypothesis that STAM1, by forming the ESCRT-0 complex with HRS, modulates endosomal sorting of activated CXCR4 in developing spinal MNs.

Dorsal projection of motor axons induced by abnormal levels of STAM1 or CXCR4

Given (1) the crucial roles of endosomal targeting of CXCR4 in facilitating CXCR4 signaling (Holleman and Marchese, 2014; Kang et al., 2014; Malik and Marchese, 2010; Marchese et al., 2003;

Sierra et al., 2010), (2) the demonstration of the importance of CXCR4 signaling in directing ventral projections of spinal motor axons (Lieberman et al., 2005) and (3) our results for the ability of STAM1 to regulate the levels of CXCR4 in developing chick spinal cord (Fig. 5), we hypothesized that STAM1 may direct ventral axonal projections of developing spinal MNs by modulating endosomal targeting of CXCR4. Specifically, we wished to examine whether knockdown of STAM1 expression mimics the aberrant dorsal projection of spinal motor axons observed in *Sdf1* and *Cxcr4* knockout mouse models (Lieberman et al., 2005). In the spinal cord, the axons of v-MNs project through the flanking paraxial mesoderm, avoiding nearby sensory ganglia (such as DRG), and establish a peripheral trajectory that lacks pre-existing axonal tracts (Wentworth, 1984). *In ovo* electroporation of si-STAM1 did not affect cell proliferation in developing chick spinal cord, as monitored by bromodeoxyuridine (BrdU) staining, in comparison with control scrambled siRNA (data not shown). To determine the trajectory pattern of motor axons with reduced levels of STAM1, we co-electroporated si-STAM1 and the *SEI*-GFP reporter, which specifically labels cell bodies and axons of MNs with GFP (Song et al., 2006). Strikingly, co-electroporation of si-STAM1 and *SEI*-GFP resulted in one or two bundles of GFP⁺ axons that project laterally to the margin of the neural tube and then reorient to a dorsal direction (Fig. 6A–C). These dorsal projection phenotypes induced by si-STAM1 were no longer observed when si-STAM1-resistant mouse STAM1 or CXCR4 was re-expressed (Fig. 6A,B). Interestingly, overexpression of STAM1 or CXCR4 also resulted in dorsal projection of GFP⁺ motor axons (Fig. 6A,B). We found that GFP⁺ motor axons are not labeled with HB9 in the dorsal spinal cord, suggesting that these GFP⁺ neurites derive from MN cell bodies located in the ventrolateral position of the spinal cord (Fig. 7). We also determined the relative distance that dorsally projecting axons traveled by measuring the length from the dorsal border of MN area to the end of the axon of dorsally projecting GFP⁺ axons (Ld) relative to the total length of the midline from the

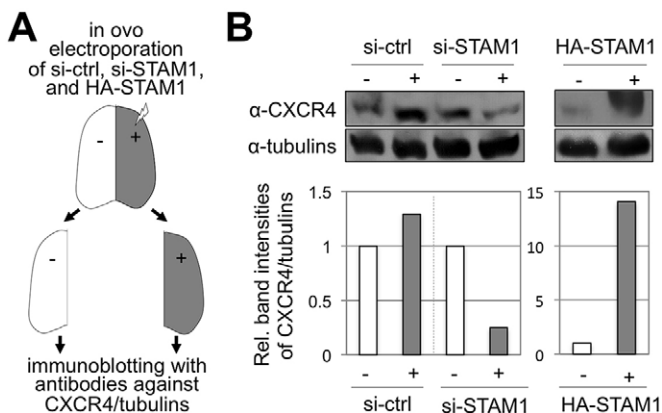


Fig. 5. Modulation of CXCR4 levels by STAM1 in the developing chick spinal cord. (A) Schematic of the experimental plan. (B) *In ovo* electroporation of si-STAM1 results in a sharp decrease in the level of CXCR4 and overexpression of STAM1 increases the level of CXCR4 in the developing chick spinal cord. Experiments were repeated independently twice.

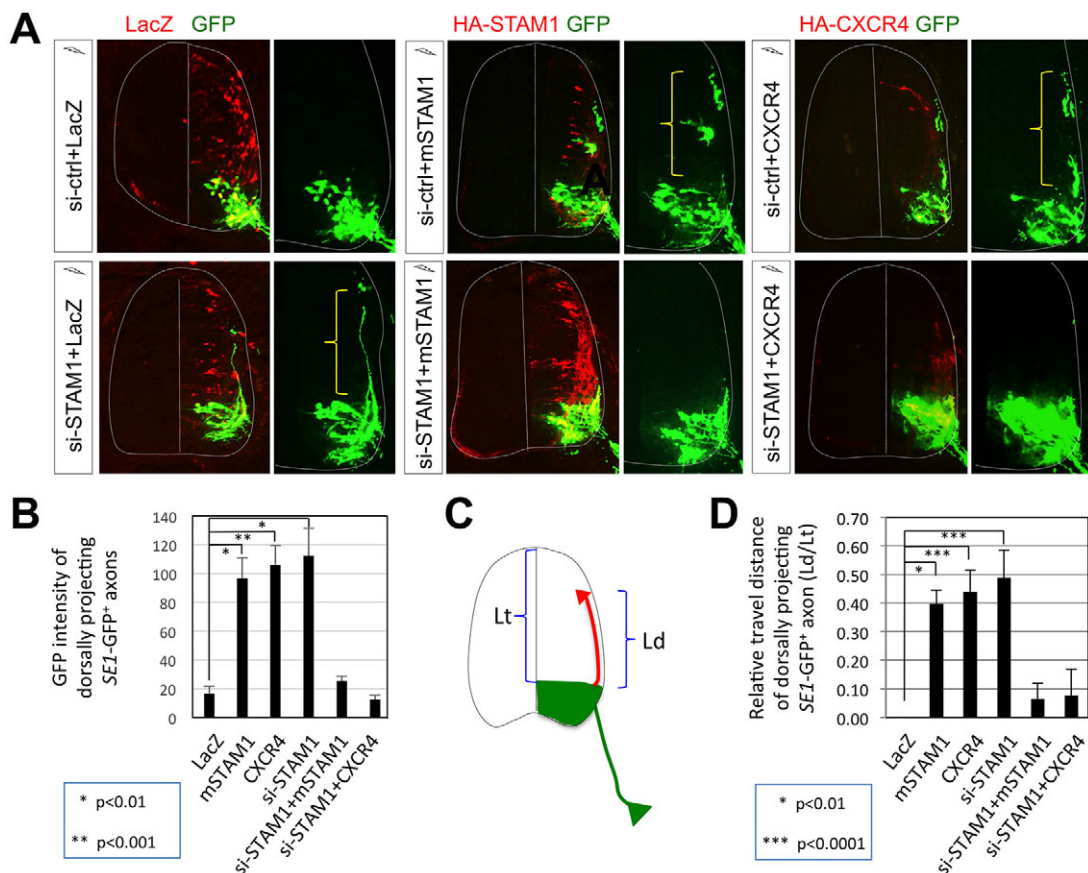


Fig. 6. STAM1 plays crucial roles in ventral exiting of spinal motor axons. (A) *In ovo* electroporation of si-control, si-STAM1, HA-mSTAM1, si-STAM1 + HA-mSTAM1, HA-CXCR4, si-STAM1+HA-CXCR4 with SE1-GFP (which specifically labels MN axons with GFP) was performed at HH13, followed by examination of GFP+ motor axonal projections. Yellow brackets indicate the area of dorsally projecting GFP+ motor axons. (B) The intensity of dorsally projecting SE1-GFP+ axons was measured using ZEN Pro 2012. (C) Schematic illustrating the direction of motor axons and distance from the MN area (green area). (D) Travel distance of dorsally projecting SE1-GFP+ axons (Ld) was measured relative to the total length of the spinal cord except the MN area (Lt). Each set of chick electroporation experiments in this figure was repeated independently at least three times with three to six embryos injected with the same combination of plasmids at each experimental set. Values are mean±s.e.m. $n=5\sim10$ independent images per sample; * $P<0.01$, ** $P<0.001$, *** $P<0.0001$, in the two-tailed *t*-test.

dorsal border of MN area to the dorsal end of the spinal cord (Lt) (Fig. 6C), and found that knockdown of STAM1 (by si-STAM1) resulted in significant dorsal projection, which was rescued by

re-expression of si-STAM1-resistant mouse STAM1 or CXCR4 (Fig. 6D). Overexpression of STAM1 or CXCR4 also resulted in significant dorsal projection (Fig. 6D). From these results, we

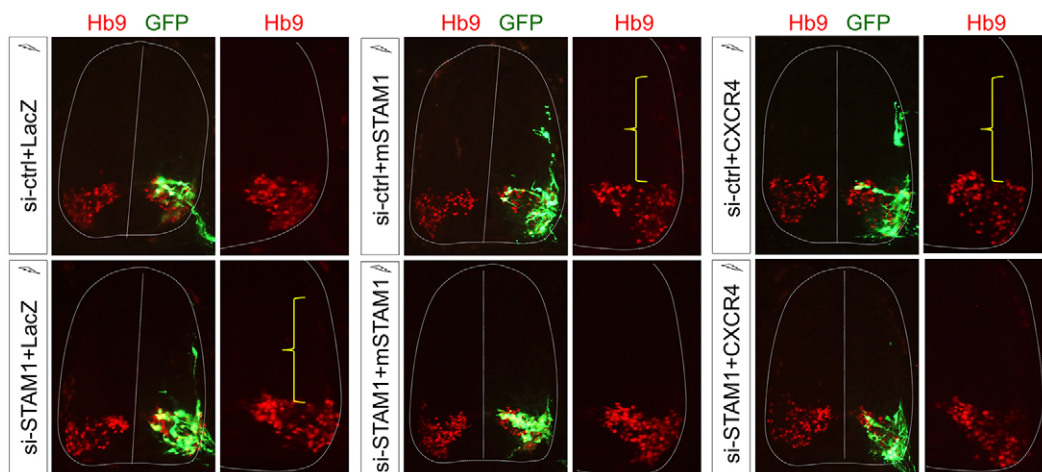


Fig. 7. Aberrant dorsally projecting motor axons. To test whether the GFP+ neurites in the dorsal spinal cord observed with knockdown of STAM1 originate from MNs that aberrantly migrate to the dorsal spinal cord, we examined the position of MN cell bodies by staining with Hb9 antibody and found that MNs do not migrate dorsally. Yellow brackets indicate the area of GFP+ neurites without ectopic MN cell bodies.

concluded that both a decrease in STAM1 levels (and the resulting decrease in CXCR4 levels) and an increase in STAM1 and CXCR4 levels cause spinal v-MNs to acquire a trajectory that shares features with the pathway of cranial d-MNs. To examine the effects of varying amounts of STAM1 and CXCR4 on motor axon projections, we electroporated the spinal cord with different amounts of STAM1 or CXCR4 alone or in combination with STAM1 knockdown. Even with a small increase in STAM1 or CXCR4 expression vector alone, we observed the aberrant axonal projection phenotype (Fig. S4). Interestingly, the aberrant dorsal motor axon projection phenotype was rescued when we electroporated the highest amounts of STAM1 or CXCR4 expression vector (Fig. S4).

Taken together, our results suggest that STAM1-directed maintenance of physiological levels of activated CXCR4 is likely to be crucial for the ventral motor axon trajectory. Because this phenotype is similar to the observation made in *Sdf1*- and *Cxcr4*-null mouse models (Lieberam et al., 2005), we propose that altered endosomal modulation of CXCR4 levels (and signaling strength) due to either reduced or elevated levels of STAM1 is at least in part responsible for the aberrant dorsal motor axonal projections.

DISCUSSION

SDF1/CXCR4 signaling has been shown to play crucial roles in ensuring ventral axonal projections of v-MNs (Lieberam et al., 2005). In this report, we presented our findings that support the roles of STAM1 in directing the ventral motor axonal projections at least in part through modulating endocytic sorting of CXCR4. First, STAM1 and HRS, two subunits of the ESCRT-0 complex, are expressed in developing MNs (Fig. 4C). Second, CXCR4 levels seem to be tightly regulated by STAM1 during MN generation, as shown by reduction of CXCR4 levels by si-STAM1 and an increase in CXCR4 levels by overexpressed STAM1 in developing spinal cord (Fig. 5). Finally, abnormal levels of CXCR4 induced by knockdown or overexpression of STAM1 results in dorsal projection of spinal motor axons (Fig. 6), similar to that observed with spinal motor axons in *Cxcr4*-null mice (Lieberam et al., 2005). These findings, along with our results demonstrating that *Stam1* is a direct target gene of the ISL1-LHX3 complex (Figs 1 and 3), suggest an important molecular pathway responsible for the ventral exiting of developing spinal motor axons, which consists of induction of STAM1 expression by the ISL1-LHX3 complex as well as subsequent formation of the ESCRT-0 complex by STAM1 and HRS and modulation of endocytic targeting of CXCR4.

By linking the ventral projections of spinal motor axons (i.e. STAM1) and the ISL1-LHX3 complex, our results support the previous prediction made from several genome-wide studies (Lee et al., 2012, 2013; Mazzoni et al., 2013) that the ISL1-LHX3 complex functions as a terminal selector of MN fate by regulating a battery of terminal differentiation genes that establish unique MN properties, such as neurogenesis, axonogenesis, axon guidance, synapse function, and cholinergic neurotransmitter characteristics (Lee et al., 2012, 2013; Cho et al., 2014). Of note, the *Stam2* gene was not associated with any ISL1-LHX3 complex-binding peak (data not shown). Interestingly, arrestin-2 has been shown to negatively modulate endosomal targeting of CXCR4 through direct interaction with STAM1 but with not its close homolog STAM2, which also forms the ESCRT-0 complex with HRS (Malik and Marchese, 2010). Accordingly, depletion of STAM1 and disruption of the arrestin-2/STAM1 interaction accelerated the degradation of CXCR4 (Malik and Marchese, 2010), which is consistent with what we observed in chick spinal cord (Fig. 5). It will be interesting to

examine further whether STAM1 plays a dominant role over STAM2 in controlling the endosomal targeting of CXCR4.

Notably, CXCR4 protein has been reported to be transiently expressed by newly generated ISL⁺ MNs soon after their migration to the lateral border of the neural tube (Lieberam et al., 2005), suggesting that CXCR4 signaling is required only for the initial ventral projections of motor axons. We speculate that STAM1 may stabilize CXCR4 proteins at the earlier developmental time point for MNs when CXCR4 is required to ensure their initial ventral axonal projections. At later stages of spinal motor axon growth, CXCR4 signaling is downregulated (Lieberam et al., 2005) and then the axonal projection may be controlled by other players such as tyrosine kinase receptor signaling systems (Ebense et al., 1996; Haase et al., 2002; Helmbacher et al., 2000). Notably, tyrosine kinase receptors are also known to be modulated by the endosomal sorting complex composed of HRS and STAM1 (Lloyd et al., 2002; Kanazawa et al., 2003), raising the possibility that STAM1 may regulate various target substrates involved in axon guidance throughout different developmental stages of spinal MN development.

Although we observed a positive correlation in protein levels between STAM1 and CXCR4 in developing chick spinal cord and HEK293 cells (Fig. 5; data not shown), it is important to note that further investigations are needed to understand the exact mechanism by which STAM1 increases the protein levels of CXCR4 in developing spinal MNs (Fig. 5) and how STAM1/CXCR4 signaling directs the initial ventral axonal projections of v-MNs (Fig. 6). It is expected that proper or homeostatic levels of STAM1 might be important to maintain appropriate levels of its target substrate proteins by either potentiating their stability or inducing their degradation through the endosomal pathway depending on different cellular contexts and upstream signaling cues. It has been shown that HRS overexpression in cells leads to HRS accumulation on early endosomes and inhibition of epidermal growth factor degradation due to the resulting impairment of the downstream degradation process (Bishop et al., 2002; Kojima et al., 2014). Interestingly, this phenotype was rescued by co-expression of exogenous STAM1, and the authors suggested that STAM1 mediates the dissociation of overexpressed HRS from the endosomal membrane, triggering reconstitution of functional ESCRT-0 for ensuing endosomal cycles (Kojima et al., 2014). These results support the notion that co-expression of a certain ratio of STAM1 and HRS, which constitute the endosomal complex ESCRT-0, is required for optimal function of the ESCRT-0 complex. Similar to the phenotypes with overexpressed HRS (Bishop et al., 2002; Kojima et al., 2014), STAM1 overexpression may also affect the recruitment and dissociation cycle of the ESCRT-0 complex, interfering with effective degradation of cargo proteins such as CXCR4. Because a decrease in STAM1 also reduces CXCR4 levels, there may be additional mechanisms such as direct control of CXCR4 stability by STAM1 via unknown mechanisms. This remains to be further investigated in the future.

Too much or too little STAM1 might affect the normal physiological condition of the cells and induce aberrant phenotypes such as dorsal axon projections of v-MNs. In understanding how STAM1/CXCR4 signaling directs the initial ventral axonal projections of v-MNs, at least two possibilities can be considered. First, CXCR4 signaling either promotes or inhibits axon outgrowth *in vitro* depending on neuronal type (Arakawa et al., 2003; Pujol et al., 2005; Xiang et al., 2002), and activation of CXCR4 signaling in certain neurons reduces the response to chemorepellent factors. Motor axon trajectories are controlled by

chemorepellent factors, such as semaphorins and netrins, secreted by floor plate cells and by the paraxial mesenchyme (Ebens et al., 1996; Haase et al., 2002; Helmbacher et al., 2000). The axons of v-MNs with activated CXCR4 signaling at the initial developmental time point may attenuate the effects of diverse repellents (Chalasan et al., 2003), enabling their ventrolateral axon extensions and exit to the periphery. Therefore, loss of CXCR4 signaling (in conjunction with STAM1 loss) would expose the axons of v-MNs to repellents in their local ventral environment, resulting in aberrant dorsal trajectories within the neural tube. SLIT, another well-known axonal repellent operates through its receptor roundabout (ROBO) (Brose and Tessier-Lavigne, 2000). It is notable that SLIT and ROBO are expressed by leukocytes, and activation of ROBO has been shown to oppose SDF1-mediated leukocyte chemotaxis (Wu et al., 2001). Interestingly, we found that SLIT3 and ROBO are highly expressed in MNs (data not shown). Therefore, it is possible that there may be cross-talk between SLIT/ROBO and SDF-1/CXCR4 signaling pathways, and that a persistently high level of activated CXCR4 signaling may inhibit the SLIT/ROBO pathway, contributing to the aberrant dorsal projection phenotypes of spinal MNs. Secondly, ESCRT-0 has been shown to direct axon pruning through downregulation of the Hedgehog receptor PATCHED (Issman-Zecharya and Schuldiner, 2014). The ESCRTs have also been shown to direct severance of the membrane necks of both axons and dendrites (Loncle et al., 2015). It is possible that these axon pruning activities of the ESCRT machinery may also be involved with the role of STAM1 in directing the ventral projection of motor axons.

In summary, our results identified STAM1 as a crucial mediator of the ventral axonal trajectory of developing spinal MNs, which probably ensures proper CXCR4 signaling through modulating the endosomal sorting of activated CXCR4. Our results also present an important regulatory axis for the ventral exiting axonal projections of developing MNs, which consists of the ISL1-LHX3-complex, STAM1 and CXCR4.

MATERIALS AND METHODS

DNA constructs

Rat *Isl1*, mouse *Lhx3* and *Ngn2*, and *lacZ* genes were cloned in pCS2 and/or pcDNA3 (Invitrogen) containing HA, Flag or myc-epitope tags for expression in mammalian cells and chick embryos, as previously described (Lee et al., 2012; Lee and Pfaff, 2003; Thaler et al., 2002). Mouse STAM1 in pcDNA3-V5-His was a gift from Dr Kazuo Sugamara (Endo et al., 2000), HA-tagged CXCR4 in pcDNA3 was a gift from Dr Adriano Marchese (Malik and Marchese, 2010) and Myc-tagged HrRS in pcDNA3 was a gift from Dr Rakesh Kumar (Rayala et al., 2006). *SE1*-GFP (Song et al., 2006) was used to label motor axons. *Stam1*-(P3-HxRE)²:LUC and *Stam1*-(P3-HxRE)⁵:GFP reporters were constructed with multiple copies of the following duplex oligonucleotides containing *Stam1*-P3-HxRE into synthetic TK-LUC or TATA-GFP vectors: sense strand 5'-GATCTTTAATTAATTAAGTTAATTAATTAATG, antisense strand 5'-GATCCATTAATTAATTAACATAATTAATTA. siRNAs for chick STAM1 with a stretch of two thymine residue overhang at the 3' end were synthesized by Integrated DNA Technologies (IDT): sense strand 5'-AUCCUUAUGGUUCACUCUCtt, antisense strand 5'-GAGAGUGA-ACCAUAAGGAUtt. Control siRNA (sc-44230) was obtained from Santa Cruz Biotechnology.

***In ovo* electroporation, IHC and ISH assays**

In ovo electroporation, line and RNA assays

In ovo electroporation was performed as described (Thaler et al., 2002). Briefly, DNAs were injected into the lumen of the neural tube of Hamburger–Hamilton (HH) stage 13 chick embryos, which were then electroporated. The embryos were harvested 3 days post-electroporation, fixed in 4% paraformaldehyde, embedded in OCT and cryosectioned at 12 μ m

thickness for IHC assays or 18 μm thickness for ISH with digoxigenin-labeled probes. Each set of chick electroporation experiments was repeated independently at least three times with three to six embryos injected with the same combination of plasmids at each experimental set. Representative sets of images from reproducible results were presented.

For IHC assays, the following antibodies were used: mouse anti-Hb9/MNR2 (Developmental Studies Hybridoma Bank, 5C10; 1:500), rabbit anti-Hb9 (Thaler et al., 1999; 1:5000), rabbit anti-Isl1/2 (Tsuchida et al., 1994; 1:2500), rabbit anti-Lhx3 (Sharma et al., 1998; 1:2000), chick anti-GFP (AVES; 1:1000), goat anti- β -galactosidase (Abcam; 1:5000), rabbit anti-STAM1 (Mizuno et al., 2004; 1:1000), rabbit anti-CXCR4 (Abcam; 1:2000) and guinea pig anti-Hrs (Lloyd et al., 2002; 1:1000). For quantification of STAM1 immunostaining (Fig. 3C) and dorsally projecting GFP-positive axons (Fig. 6B), we used ZEN Pro 2012 (Zeiss) to measure the intensity of FITC signal of different regions in the spinal cord.

For ISH analyses, cDNA for chick *Stam1* was purchased from ARK genomics. Chick *CXCR4* (11-458 bp) and chick *CXCR7* (125-526 bp) were cloned to pBluescript vector and used to generate digoxigenin-labeled riboprobe.

Mice

The generation of *Hb9*^{-/-};*Isl2*^{-/-} dKO mice has been described previously (Thaler et al., 2004). *Hb9*^{+/-};*Isl2*^{+/-} male mice were crossed with *Hb9*^{+/-};*Isl2*^{+/-} female mice to get dKO mutant embryos for the analyses. Mouse embryos were collected at the indicated developmental stages, and processed similarly to chick embryos as described above.

Luciferase reporter assays

P19 embryonic carcinoma cells were cultured in MEM supplemented with 10% fetal bovine serum. For luciferase assays, P19 cells were plated in 48-well plates and incubated for 24 h, followed by transient transfections using Lipofectamine 2000 (Invitrogen). An actin- β -galactosidase plasmid was co-transfected for normalization of transfection efficiency and empty vectors were used to equalize the total amount of DNA. Cells were harvested 36–40 h after transfection. Cell extracts were assayed for luciferase activity and the values were normalized with β -galactosidase activity. All transfections were repeated independently at least three times. Data are represented as the mean of triplicate values obtained from representative experiments. Error bars represent standard deviation.

Co-immunoprecipitation assays and immunoblotting assays

HEK293 cells were cultured in DMEM media supplemented with 10% fetal bovine serum. For co-immunoprecipitation, HEK293 cells were seeded on 10-cm tissue culture dishes, cultured in DMEM media supplemented with 10% fetal bovine serum, and transfected with the expression vectors for Flag-STAM1, Myc-Hrs, and HA-CXCR4 using Superfect (Qiagen). Two days after transfection, cells were treated with hSDF1 (50 ng/ml, Peprotech) for 30 min and then cells were harvested and lysed in IP buffer (20 mM Tris-HCl, pH 8.0, 0.5% NP-40, 1 mM EDTA, 150 mM NaCl, 2 mM PMSF, 10% glycerol, 4 mM Na₃VO₄, 200 mM NaF, 20 mM Na-pyrophosphate, and protease inhibitor cocktail). In these studies, immunoprecipitations were performed with mouse anti-HA antibody (MMS-101R, Covance). The interactions were monitored by western blotting assays using mouse anti-Flag (F3165, Sigma; 1:5000) and mouse anti-Myc (9E10, Millipore; 1:5000) antibodies. To detect chick CXCR4 protein level in si-STAM1-electroporated chick spinal cord extract, rabbit anti-CXCR4 (ab2074, Abcam; 1:2000) and rabbit anti-β-tubulin (sc-9104, Santa Cruz; 1:2000) antibodies were used for immunoblotting assays.

Immunostaining in primary MNs and HEK293 cells

HEK293 cells were transfected and treated with hSDF1 as above. Primary MNs were isolated from E9.5 wild-type ICR mice and cultured for 24 h following the reported protocol (Gingras et al., 2007). To examine the colocalization, cells were stained with mouse anti-Myc (9E10, Millipore; 1:5000), rabbit anti-HA (sc-805, Santa Cruz; 1:200), rabbit anti-STAM1 (12434-1-AP, Proteintech Group; 1:1000), mouse anti-EEA1 (610457, BD Transduction Laboratory; 1:1000) and rabbit anti-CXCR4 (ab2074, Abcam; 1:2000) antibodies.

RNA extraction and quantitative RT-PCR

P19 cells were transfected with ISL1, LHX3 and NGN2 using Lipofectamine 2000 (Invitrogen) and 72 h later cells were harvested for RNA extraction. Total RNAs were extracted using Trizol (Invitrogen) and reverse transcribed using the SuperScript III First-Strand Synthesis System (Invitrogen). The levels of mRNA were determined by quantitative RT-PCR using SYBR-Green Kit (Invitrogen) and CFX Connect Real-Time PCR detection system (Bio-Rad). The following primers were used: mouse *Hb9*, 5'-GTTGGAGCTGGAACACCAGT, 5'-CTTTTGCTGCGTTCCATT; mouse *Stam1*, 5'-CTGCAGATCTTACTGCTGAACC, 5'-TCAAGATGAAGCAGCTCTGG; and cyclophilin A, 5'-GTCTCCTTCGAGCTGTTTG-C, 5'-GATGCCAGGACCTGTATGCT. Data are shown as the mean of duplicate values obtained from representative experiments. Error bars represent standard deviation.

ChIP assays

ChIP was performed in mouse embryonic spinal cords as described previously (Cho et al., 2014; Lee et al., 2013). The spinal cords were microdissected from E12.5 mouse embryos and cells were dissociated and subjected to ChIP assays. Cells were washed with PBS buffer, fixed in 1% formaldehyde for 10 min at room temperature, and quenched with 125 mM glycine. Cells were washed with Buffer I (0.25% Triton X-100, 10 mM EDTA, 0.5 mM EGTA, 10 mM HEPES, pH 6.5) and Buffer II (200 mM NaCl, 1 mM EDTA, 0.5 mM EGTA, 10 mM HEPES, pH 6.5) sequentially. Then, cells were lysed with lysis buffer (0.5% SDS, 5 mM EDTA, 50 mM Tris-HCl, pH 8.0, protease inhibitor mixture) and were subjected to sonication for DNA shearing. Next, cell lysates were diluted 1:10 in ChIP buffer (0.5% Triton X-100, 2 mM EDTA, 100 mM NaCl, 50 mM Tris-HCl, pH 8.0, protease inhibitor mixture) and, for immunoclearing, were incubated with IgG and protein A agarose beads (15918-014, Invitrogen) for 1 h at 4°C. The supernatant was collected after a quick spin and incubated with anti-IgG (I-5381, Sigma), anti-Is11 (Tsuchida et al., 1994) and anti-Lhx3 (Sharma et al., 1998) antibodies and protein A agarose beads to precipitate the ISL1-LHX3 complex/chromatin complex overnight at 4°C. After pull-down of the ISL1-LHX3/chromatin/antibody complex with protein A agarose beads, the beads were washed with TSE I (0.1% SDS, 1% Triton X-100, 2 mM EDTA, 20 mM Tris-HCl, pH 8.0, 150 mM NaCl), TSE II (same components as in TSE I except 500 mM NaCl) and Buffer III (0.25 M LiCl, 1% Nonidet P-40, 1% deoxycholate, 1 mM EDTA, 10 mM Tris-HCl, pH 8.0) sequentially for 10 min at each step. Then the beads were washed with Tris-EDTA (TE) buffer three times. ISL1-LHX3/chromatin complexes were eluted in elution buffer (1% SDS, 1 mM EDTA, 0.1 M NaHCO₃, 50 mM Tris-HCl, pH 8.0) and de-crosslinked by incubating at 65°C overnight. The eluate was incubated at 50°C for at least 2 h with Proteinase K. Next, DNA was purified with phenol/chloroform and the DNA pellet was precipitated by ethanol and resolved in water. The purified final DNA samples were subjected to quantitative PCR reactions. The primers used for ChIP-PCR were: *Hb9*-MN enhancer, forward, 5'-TACTCTCCC-TACAGTCTCTGGGGT, reverse, 5'-TGTCCAGAAATCCACAGGCCT-GCG; *Stam1*-P1, forward, 5'-TGCTAGGTAACAACCTAACAATTT, reverse, 5'-CTTCCCACATATTGGTATGGGAAGC; *Stam1*-P2, forward, 5'-TCAGTGTCTAAATGCTGAGCAGTA, reverse, 5'-GACAAAGAAA-CAAAGGCAGAGAAT; *Stam1*-P3, forward, 5'-AGTGTGCACTAAAG-TATGGAAAGC, reverse, 5'-ATAAGCGATGTGCACGTAGGTCA; *Stam1*-P4, forward, 5'-TCCTATGCTCCCTTGTTACAAATC, reverse, 5'-CTGACAGTGATTGTGAGCAGGCAT; *Stam1*-P5, forward, 5'-GATGG-AAGAAACAGAAATGATCC, reverse, 5'-CAATCTCATCATCATG-TTCGAGA; and *Untr6*, forward, 5'-TCAGGCATGAACCATCATAC, reverse, 5'-AACATCCACACGTCCAGTGA.

Acknowledgements

We thank Dr Soo-Kyung Lee (OHSU, Portland, USA) for reagents and many helpful suggestions during the course of this work, as well as Drs Soo-Kyung Lee and Jae W. Lee (OHSU, Portland, USA) for critically reading the manuscript. We also thank Drs Kazuo Sugamura, Adriano Marchese, Masayuki Komada, Hugo J. Bellen and Rakesh Kumar for various reagents.

Competing interests

The authors declare no competing or financial interests.

Author contributions

S.L. conceived and designed the experiments and wrote the manuscript. S.L. and H.N. performed experiments and data analysis.

Funding

This research was supported by Basic Science Research Program [NRF-2015R1A2A1A15055611 to S.L.] and Bio & Medical Technology Development Program [NRF-2012M3A9C6050508 to S.L.] and the Global Core Research Center (GCRC) [2011-0030001 to S.L.] through the National Research Foundation of Korea (NRF) funded by the Ministry of Science, ICT and Future Planning (MSIP).

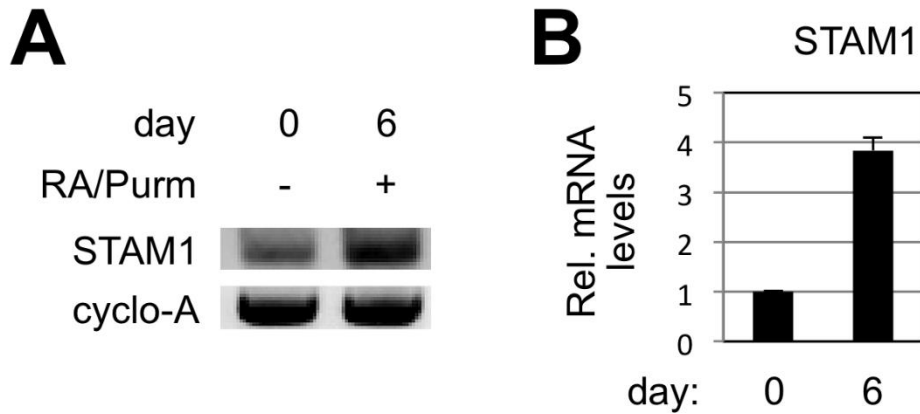
Supplementary information

Supplementary information available online at <http://dev.biologists.org/lookup/doi/10.1242/dev.135848.supplemental>

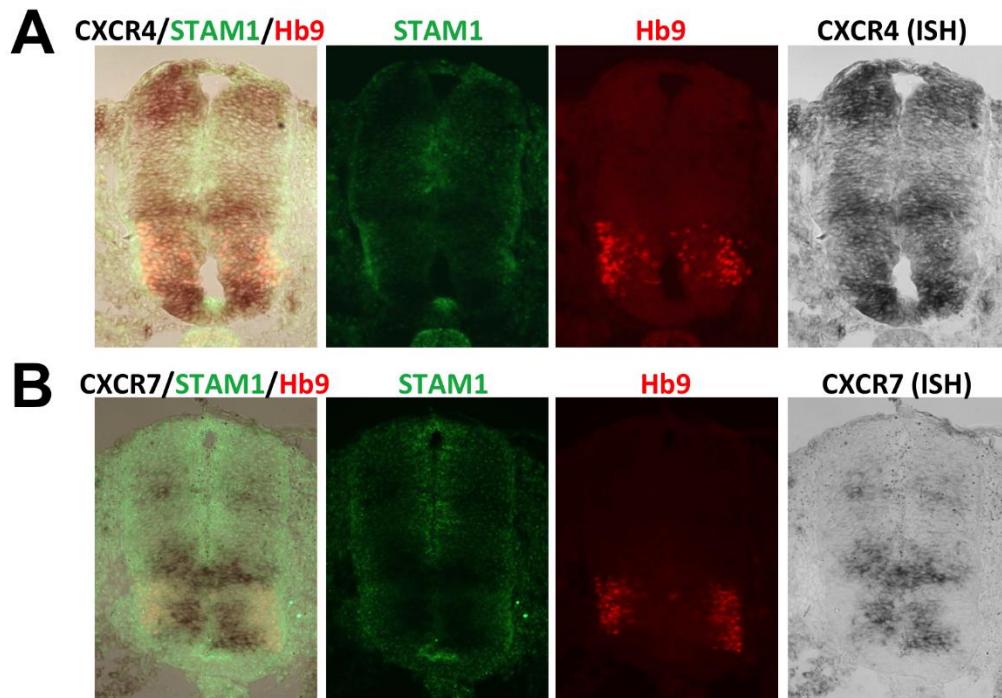
References

- Arakawa, Y., Bito, H., Furuyashiki, T., Tsuji, T., Takemoto-Kimura, S., Kimura, K., Nozaki, K., Hashimoto, N. and Narumiya, S. (2003). Control of axon elongation via an SDF-1alpha/Rho/mDia pathway in cultured cerebellar granule neurons. *J. Cell Biol.* **161**, 381–391.
- Bache, K. G., Raiborg, C., Mehlum, A. and Stenmark, H. (2003). STAM and Hrs are subunits of a multivalent ubiquitin-binding complex on early endosomes. *J. Biol. Chem.* **278**, 12513–12521.
- Bhandari, D., Trejo, J., Benovic, J. L. and Marchese, A. (2007). Arrestin-2 interacts with the ubiquitin-protein isopeptide ligase atrophin-interacting protein 4 and mediates endosomal sorting of the chemokine receptor CXCR4. *J. Biol. Chem.* **282**, 36971–36979.
- Bishop, N., Horman, A. and Woodman, P. (2002). Mammalian class E vps proteins recognize ubiquitin and act in the removal of endosomal protein-ubiquitin conjugates. *J. Cell Biol.* **157**, 91–102.
- Brose, K. and Tessier-Lavigne, M. (2000). Slit proteins: key regulators of axon guidance, axonal branching, and cell migration. *Curr. Opin. Neurobiol.* **10**, 95–102.
- Chalasani, S. H., Sabelko, K. A., Sunshine, M. J., Littman, D. R. and Raper, J. A. (2003). A chemokine, SDF-1, reduces the effectiveness of multiple axonal repellents and is required for normal axon pathfinding. *J. Neurosci.* **23**, 1360–1371.
- Cho, H.-H., Carnagin, F., Kim, Y., Lee, B., Kwon, R.-J., Nam, H., Shen, R., Barnes, A. P., Lee, J. W., Lee, S. et al. (2014). Isl1 directly controls a cholinergic neuronal identity in the developing forebrain and spinal cord by forming cell type-specific complexes. *PLoS Genet.* **10**, e1004280.
- Ebner, A., Brose, K., Leonardo, E. D., Hanson, M. G., Jr., Blatt, F., Birchmeier, C., Barres, B. A. and Tessier-Lavigne, M. (1996). Hepatocyte growth factor/scatter factor is an axonal chemoattractant and a neurotrophic factor for spinal motor neurons. *Neuron* **17**, 1157–1172.
- Endo, K., Takeshita, T., Kasai, H., Sasaki, Y., Tanaka, N., Asao, H., Kikuchi, K., Yamada, M., Chenb, M., O'Shea, J. J. et al. (2000). STAM2, a new member of the STAM family, binding to the Janus kinases. *FEBS Lett.* **477**, 55–61.
- Gingras, M., Gagnon, V., Minotti, S., Durham, H. D. and Berthod, F. (2007). Optimized protocols for isolation of primary motor neurons, astrocytes and microglia from embryonic mouse spinal cord. *J. Neurosci. Methods* **163**, 111–118.
- Guthrie, S. and Lumsden, A. (1992). MN pathfinding following rhombomere reversals in the chick embryo hindbrain. *Development* **114**, 663–673.
- Haase, G., Dessaud, E., Garcès, A., de Bovis, B., Birling, M.-C., Filippi, P., Schmalbruch, H., Arber, S. and deLapeyriere, O. (2002). GDNF acts through PEA3 to regulate cell body positioning and muscle innervation of specific motor neuron pools. *Neuron* **35**, 893–905.
- Helmbacher, F., Schneider-Maunoury, S., Topilko, P., Turet, L. and Charnay, P. (2000). Targeting of the EphA4 tyrosine kinase receptor affects dorsal/ventral pathfinding of limb motor axons. *Development* **127**, 3313–3324.
- Henne, W. M., Stenmark, H. and Emr, S. D. (2013). Molecular mechanisms of the membrane sculpting ESCRT pathway. *Cold Spring Harb. Perspect. Biol.* **5**, a016766.
- Holleman, J. and Marchese, A. (2014). The ubiquitin ligase deltex-3l regulates endosomal sorting of the G protein-coupled receptor CXCR4. *Mol. Biol. Cell* **25**, 1892–1904.
- Hurley, J. H. (2015). ESCRTs are everywhere. *EMBO J.* **34**, 2398–2407.
- Issman-Zecharya, N. and Schuldiner, O. (2014). The PI3K class III complex promotes axon pruning by downregulating a Ptc-derived signal via endosome-lysosomal degradation. *Dev. Cell* **31**, 461–473.
- Kanazawa, C., Morita, E., Yamada, M., Ishii, N., Miura, S., Asao, H., Yoshimori, T. and Sugamura, K. (2003). Effects of deficiencies of STAMs and Hrs, mammalian class E Vps proteins, on receptor downregulation. *Biochem. Biophys. Res. Commun.* **309**, 848–856.
- Kang, D. S., Tian, X. and Benovic, J. L. (2014). Role of beta-arrestins and arrestin domain-containing proteins in G protein-coupled receptor trafficking. *Curr. Opin. Cell Biol.* **27**, 63–71.
- Kennedy, J. E. and Marchese, A. (2015). Regulation of GPCR trafficking by ubiquitin. *Prog. Mol. Biol. Transl. Sci.* **132**, 15–38.

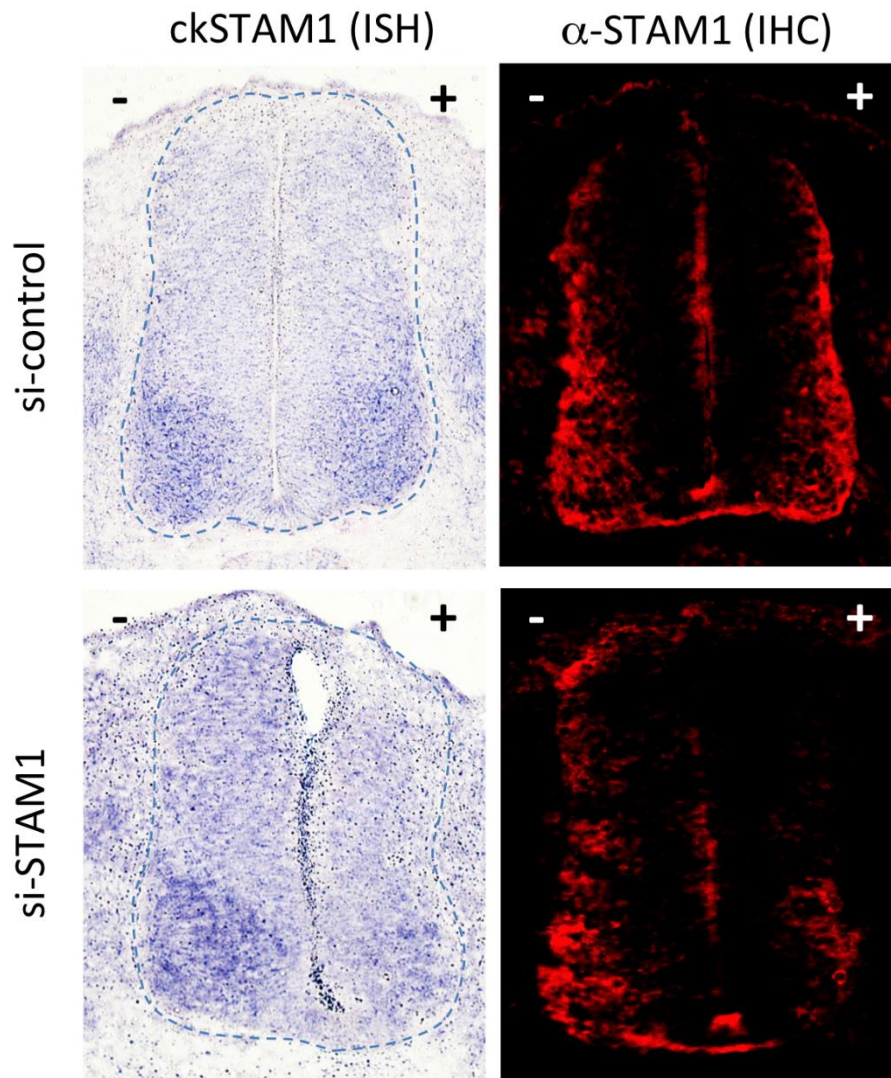
- Kobayashi, H., Tanaka, N., Asao, H., Miura, S., Kyuuma, M., Semura, K., Ishii, N. and Sugamura, K. (2005). Hrs, a mammalian master molecule in vesicular transport and protein sorting, suppresses the degradation of ESCRT proteins signal transducing adaptor molecule 1 and 2. *J. Biol. Chem.* **280**, 10468-10477.
- Kojima, K., Amano, Y., Yoshino, K., Tanaka, N., Sugamura, K. and Takeshita, T. (2014). ESCRT-0 protein hepatocyte growth factor-regulated tyrosine kinase substrate (Hrs) is targeted to endosomes independently of signal-transducing adaptor molecule (STAM) and the complex formation with STAM promotes its endosomal dissociation. *J. Biol. Chem.* **289**, 33296-33310.
- Kolodkin, A. L. and Tessier-Lavigne, M. (2011). Mechanisms and molecules of neuronal wiring: a primer. *Cold Spring Harb. Perspect. Biol.* **3**, a001727.
- Lee, S.-K. and Pfaff, S. L. (2003). Synchronization of neurogenesis and motor neuron specification by direct coupling of bHLH and homeodomain transcription factors. *Neuron* **38**, 731-745.
- Lee, S., Lee, B., Joshi, K., Pfaff, S. L., Lee, J. W. and Lee, S.-K. (2008). A regulatory network to segregate the identity of neuronal subtypes. *Dev. Cell* **14**, 877-889.
- Lee, S., Cuvillier, J. M., Lee, B., Shen, R., Lee, J. W. and Lee, S.-K. (2012). Fusion protein Isl1-Lhx3 specifies motor neuron fate by inducing motor neuron genes and concomitantly suppressing the interneuron programs. *Proc. Natl. Acad. Sci. USA* **109**, 3383-3388.
- Lee, S., Shen, R., Cho, H.-H., Kwon, R.-J., Seo, S. Y., Lee, J. W. and Lee, S.-K. (2013). STAT3 promotes motor neuron differentiation by collaborating with motor neuron-specific LIM complex. *Proc. Natl. Acad. Sci. USA* **110**, 11445-11450.
- Lieberam, I., Agalliu, D., Nagasawa, T., Ericson, J. and Jessell, T. M. (2005). A Cxcl12-CXCR4 chemokine signaling pathway defines the initial trajectory of mammalian motor axons. *Neuron* **47**, 667-679.
- Lloyd, T. E., Atkinson, R., Wu, M. N., Zhou, Y., Pennetta, G. and Bellen, H. J. (2002). Hrs regulates endosome membrane invagination and tyrosine kinase receptor signaling in *Drosophila*. *Cell* **108**, 261-269.
- Loncle, N., Agromayor, M., Martin-Serrano, J. and Williams, D. W. (2015). An ESCRT module is required for neuron pruning. *Sci. Rep.* **5**, 8461.
- Mali, R. S., Peng, G.-H., Zhang, X., Dang, L., Chen, S. and Mitton, K. P. (2008). FIZ1 is part of the regulatory protein complex on active photoreceptor-specific gene promoters in vivo. *BMC Mol. Biol.* **9**, 87.
- Malik, R. and Marchese, A. (2010). Arrestin-2 interacts with the endosomal sorting complex required for transport machinery to modulate endosomal sorting of CXCR4. *Mol. Biol. Cell* **21**, 2529-2541.
- Marchese, A., Raiborg, C., Santini, F., Keen, J. H., Stenmark, H. and Benovic, J. L. (2003). The E3 ubiquitin ligase ALP4 mediates ubiquitination and sorting of the G protein-coupled receptor CXCR4. *Dev. Cell* **5**, 709-722.
- Mazzoni, E. O., Mahony, S., Closser, M., Morrison, C. A., Nedelec, S., Williams, D. J., An, D., Gifford, D. K. and Wichterle, H. (2013). Synergistic binding of transcription factors to cell-specific enhancers programs motor neuron identity. *Nat. Neurosci.* **16**, 1219-1227.
- Mizuno, E., Kawahata, K., Kato, M., Kitamura, N. and Komada, M. (2003). STAM proteins bind ubiquitinated proteins on the early endosome via the VHS domain and ubiquitin-interacting motif. *Mol. Biol. Cell* **14**, 3675-3689.
- Mizuno, E., Kawahata, K., Okamoto, A., Kitamura, N. and Komada, M. (2004). Association with Hrs is required for the early endosomal localization, stability, and function of STAM. *J. Biochem.* **135**, 385-396.
- Mu, F.-T., Callaghan, J. M., Steele-Mortimer, O., Stenmark, H., Parton, R. G., Campbell, P. L., McCluskey, J., Yeo, J.-P., Tock, E. P. C. and Toh, B.-H. (1995). EEA1, an early endosome-associated protein. EEA1 is a conserved alpha-helical peripheral membrane protein flanked by cysteine "fingers" and contains a calmodulin-binding IQ motif. *J. Biol. Chem.* **270**, 13503-13511.
- Niederlander, C. and Lumsden, A. (1996). Late emigrating neural crest cells migrate specifically to the exit points of cranial branchiomotor nerves. *Development* **122**, 2367-2374.
- Ödemis, V., Lamp, E., Pezeszki, G., Moepps, B., Schilling, K., Gierschik, P., Littman, D. R. and Engele, J. (2005). Mice deficient in the chemokine receptor CXCR4 exhibit impaired limb innervation and myogenesis. *Mol. Cell. Neurosci.* **30**, 494-505.
- Pfaff, S. L., Mendelsohn, M., Stewart, C. L., Edlund, T. and Jessell, T. M. (1996). Requirement for LIM homeobox gene Isl1 in motor neuron generation reveals a motor neuron-dependent step in interneuron differentiation. *Cell* **84**, 309-320.
- Pujol, F., Kitabgi, P. and Boudin, H. (2005). The chemokine SDF-1 differentially regulates axonal elongation and branching in hippocampal neurons. *J. Cell Sci.* **118**, 1071-1080.
- Rayala, S. K., den Hollander, P., Balasenthil, S., Molli, P. R., Bean, A. J., Vadlamudi, R. K., Wang, R.-A. and Kumar, R. (2006). Hepatocyte growth factor-regulated tyrosine kinase substrate (HRS) interacts with PELP1 and activates MAPK. *J. Biol. Chem.* **281**, 4395-4403.
- Sapède, D., Rossel, M., Dambly-Chaudière, C. and Ghysen, A. (2005). Role of SDF1 chemokine in the development of lateral line efferent and facial motor neurons. *Proc. Natl. Acad. Sci. USA* **102**, 1714-1718.
- Sharma, K., Sheng, H. Z., Lettieri, K., Li, H., Karavanov, A., Potter, S., Westphal, H. and Pfaff, S. L. (1998). LIM homeodomain factors Lhx3 and Lhx4 assign subtype identities for motor neurons. *Cell* **95**, 817-828.
- Sierra, M. I., Wright, M. H. and Nash, P. D. (2010). AMSH interacts with ESCRT-0 to regulate the stability and trafficking of CXCR4. *J. Biol. Chem.* **285**, 13990-14004.
- Song, M.-R., Shirasaki, R., Cai, C.-L., Ruiz, E. C., Evans, S. M., Lee, S.-K. and Pfaff, S. L. (2006). T-Box transcription factor Tbx20 regulates a genetic program for cranial motor neuron cell body migration. *Development* **133**, 4945-4955.
- Tanabe, Y., William, C. and Jessell, T. M. (1998). Specification of motor neuron identity by the MNR2 homeodomain protein. *Cell* **95**, 67-80.
- Thaler, J., Harrison, K., Sharma, K., Lettieri, K., Kehrl, J. and Pfaff, S. L. (1999). Active suppression of interneuron programs within developing motor neurons revealed by analysis of homeodomain factor HB9. *Neuron* **23**, 675-687.
- Thaler, J. P., Lee, S.-K., Jurata, L. W., Gill, G. N. and Pfaff, S. L. (2002). LIM factor Lhx3 contributes to the specification of motor neuron and interneuron identity through cell-type-specific protein-protein interactions. *Cell* **110**, 237-249.
- Thaler, J. P., Koo, S. J., Kania, A., Lettieri, K., Andrews, S., Cox, C., Jessell, T. M. and Pfaff, S. L. (2004). A postmitotic role for Isl-class LIM homeodomain proteins in the assignment of visceral spinal motor neuron identity. *Neuron* **41**, 337-350.
- Tosney, K. W. and Landmesser, L. T. (1985). Specificity of early motoneuron growth cone outgrowth in the chick embryo. *J. Neurosci.* **5**, 2336-2344.
- Tsuchida, T., Ensini, M., Morton, S. B., Baldassarre, M., Edlund, T., Jessell, T. M. and Pfaff, S. L. (1994). Topographic organization of embryonic motor neurons defined by expression of LIM homeobox genes. *Cell* **79**, 957-970.
- Wentworth, L. E. (1984). The development of the cervical spinal cord of the mouse embryo. I. A Golgi analysis of ventral root neuron differentiation. *J. Comp. Neurol.* **222**, 81-95.
- Wichterle, H., Lieberam, I., Porter, J. A. and Jessell, T. M. (2002). Directed differentiation of embryonic stem cells into motor neurons. *Cell* **110**, 385-397.
- Wu, J. Y., Feng, L., Park, H.-T., Havlioglu, N., Wen, L., Tang, H., Bacon, K. B., Jiang, Z.-h., Zhang, X.-c. and Rao, Y. (2001). The neuronal repellent Slit inhibits leukocyte chemotaxis induced by chemotactic factors. *Nature* **410**, 948-952.
- Xiang, Y., Li, Y., Zhang, Z., Cui, K., Wang, S., Yuan, X.-b., Wu, C.-p., Poo, M.-m. and Duan, S. (2002). Nerve growth cone guidance mediated by G protein-coupled receptors. *Nat. Neurosci.* **5**, 843-848.
- Yamada, M., Takeshita, T., Miura, S., Murata, K., Kimura, Y., Ishii, N., Nose, M., Sakagami, H., Kondo, H., Tashiro, F. et al. (2001). Loss of hippocampal CA3 pyramidal neurons in mice lacking STAM1. *Mol. Cell. Biol.* **21**, 3807-3819.
- Yamada, M., Ishii, N., Asao, H., Murata, K., Kanazawa, C., Sasaki, H. and Sugamura, K. (2002). Signal-transducing adaptor molecules STAM1 and STAM2 are required for T-cell development and survival. *Mol. Cell. Biol.* **22**, 8648-8658.



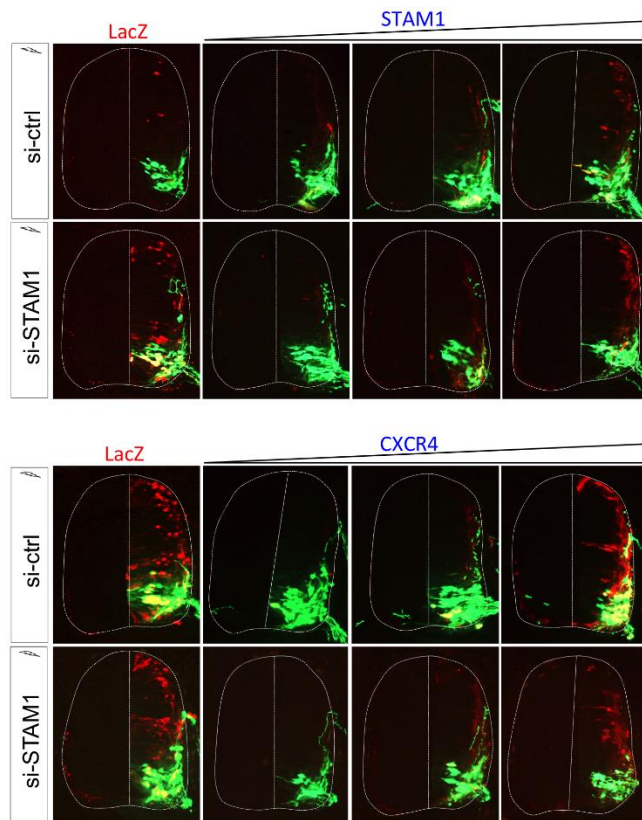
S-Fig. 1. Induction of STAM1 in developing MNs. (A) Expression of higher levels of STAM1 in MNs derived from mouse embryonic stem cells (ESCs) in comparison to proliferating ESCs as determined by RT-PCR. The ESC line was maintained in an undifferentiated state on 0.1% gelatin-coated dishes in the ESC growth media that consist of knockout DMEM, 10% FBS, 0.1 mM nonessential amino acids, 2 mM L-glutamine, 0.1 mM β -mercaptoethanol, and recombinant leukemia inhibitory factor (LIF) (1,000 units/ml, Chemicon). For MN differentiation assays, ESCs were trypsinized and grown in the ESC growth medium without LIF in suspension as cell aggregates for two days. The ESC aggregates (embryoid bodies, EBs) were treated with all-trans RA (0.5 μ M) and a Shh agonist Purmorphamine (1 μ M, Calbiochem) for 4 days. (B) Quantification of the RT-PCR results is as shown.



S-Fig. 2. Expression of CXCR4 and CXCR7 in developing chick spinal cord. (A) CXCR4 is expressed highly at early stage of chick embryonic spinal cord (HH18) and some of the signals overlap with Hb9 and STAM1 in motor neuron area. In situ hybridization (ISH) is used for CXCR4 expression followed by immunohistochemistry for Hb9 and STAM1 and the merged image is as shown. (B) ISH shows the expression of CXCR7 in the ventricular zone of chick spinal cord and this CXCR7 expression is excluded from the motor neuron area.



S-Fig. 3. Validation of si-STAM1. To test the knock-down efficiency of si-STAM1, chick neural tubes were electroporated with si-control and si-STAM1, followed by in situ hybridization (ISH) against chick STAM1 and immunohistochemistry with anti-STAM1 antibody at two days post-electroporation (2dpe). +, electroporated side.



S-Fig. 4. Varying amount of STAM1 and CXCR4 affects motor axon projections. Increasing the expression of STAM1 or CXCR4 alone results in *SE1*-GFP labeled motor axons to project dorsally. This phenotype is rescued when the expression of STAM1 or CXCR4 is increased maximally, suggesting that a specific dose is required for both STAM1 and CXCR4 for proper ventral motor axon outgrowth.